Uncertainty and Sensitivity Analysis of the SF Source Term of I-129 in the MELODIE Model using SUSA

GRS - 314

Gesellschaft für Anlagen-
und Reaktorsicherheit
(GRS) mbH

Uncertainty and Sensitivity Analysis of the SF Source Term of I-129 in the MELODIE Model using SUSA

Guido Bracke
Stephan Hotzel
Gregory Mathieu

September 2009

Remark:

Work performed as part of the European Atomic Energy Community‘s R&T programme on Nuclear Energy 2002 - 2006, Area: Management of Radioactive Waste, Contract No.: FI6W-036366.

The work was conducted by the Gesellschaft für Anlagen- und Reaktorsicherheit (GRS) mbH and the Institut de Radioprotection et de Sûreté Nucléaire (IRSN).

The authors are responsible for the content of the report.

GRS - 314
ISBN 978-3-939355-93-9

Keywords

Degradation, Dissolution, Final Disposal, Inventory, Iodine-129, IRF, MELODIE, Probability Distribution Function, Radionuclide Release, Spent Fuel, SUSA, Transport, Uncertainty Analysis

Content

1 Introduction

The uncertainty and sensitivity of spent fuel degradation models on the release of radionuclides is studied by GRS and IRSN in the following report. An important part is to correlate the uncertainties in the assumptions made for simulating the spent fuel degradation and the uncertainties in the associated release of radionuclides and to determine the sensitivity of the parameters by a probabilistic method. Sensitivity analysis was performed already using deterministic calculations in the french case /AND 05/.

GRS and IRSN have decided to model the concept based on the ANDRA's Carbon steel SF/Iron/Clay concept /NF 05/ as a test case. Spent fuel canisters are disposed of in horizontal tunnels closed by a bentonite plug. A bentonite buffer is placed around the canisters. Bentonite seals close the access drifts in order to limit the water flow in the repository. GRS/IRSN decided to use I-129 as an example for the release and transport.

The probabilistic approach is applied by GRS to address uncertainty propagation on radionuclide release and transport and to analyze the sensitivity varying selected parameter values in accordance with their probabilistic density distribution.

The strategy for probabilistic calculations consists of three steps:

1. The selection of parameters and their probabilistic density distribution and generation of the data set with the software SUSA for the calculation of 100 model realizations.
2. Using the parameter set to calculate the activity flows at 4 indicators for each realization with the MELODIE software.
3. Analysis of the results of the MELODIE software by GRS using SUSA for uncertainty and sensitivity.

2 The MELODIE model

The MELODIE software performs 3D saturated flow and transport calculations using numerical methods. It is described in some detail elsewhere /MAT 08/. The following figures show the model used. Fig. 2.1 depicts a disposal tunnel of spent fuel in a clayey host rock. The spent fuel is disposed horizontally in the tunnel. The tunnel is sealed with a bentonite plug and concrete. Fig. 2.2 depicts the flows which are imposed in the model. The upward flow is set to 1E-6 m/y whereas the flow exiting the disposal tunnel is up to 1E-3 m/y. Fig. 2.3 depicts a sketch of the indicator locations given as activity fluxes through surfaces. Indicator 1 (Phi 1) is the total activity flux from the surface of the disposal tunnel to the host rock (black arrows). Indicator 2 (Phi 2) is the activity flux from the disposal tunnel through the surface of the bentonite plug and concrete to the drift (blue arrow). Indicator 3 (Phi 3) is the activity flux through the top surface of the host rock (green arrow) into the upper aquifer. Indicator 4 (Phi 4) is the activity flux through the bottom surface of the host rock (red arrow).

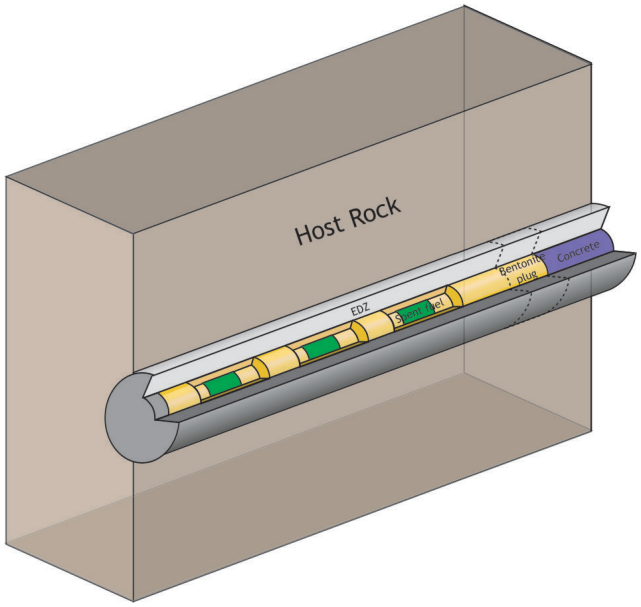

Fig. 2.1 Sketch of the simulation model representing a disposal tunnel of spent fuel

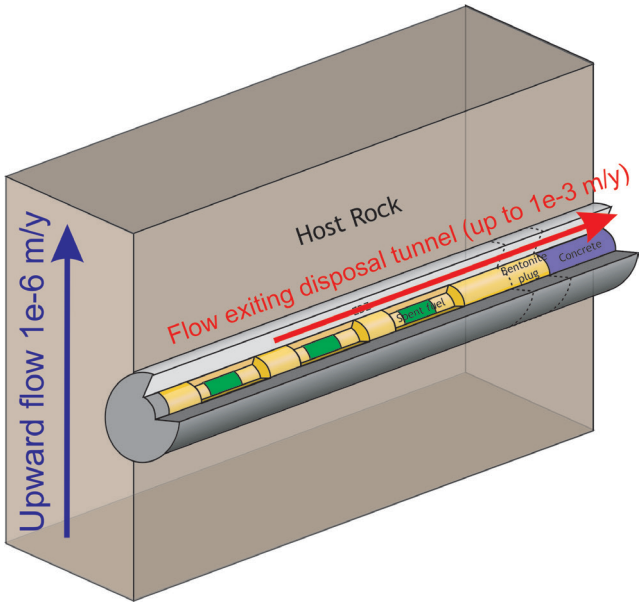

Fig. 2.2 Sketch of the upward flow imposed in the model

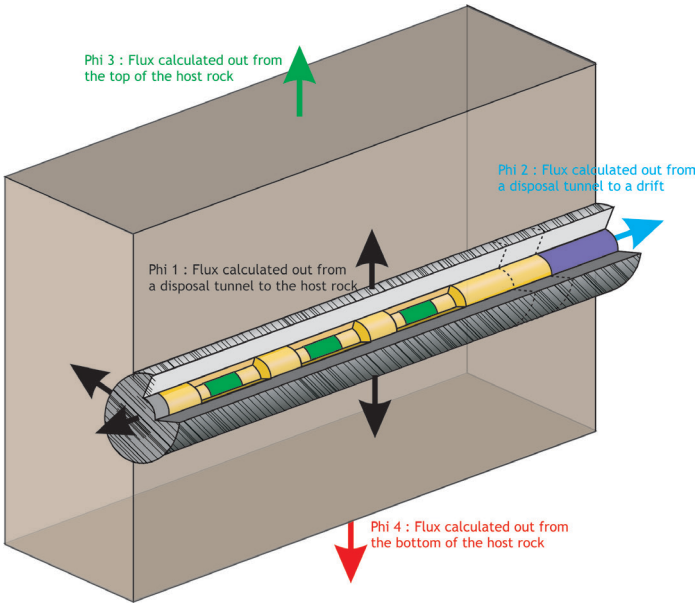

Fig. 2.3 Sketch of the indicator locations (activity fluxes here) used to assess the system performance

3 SUSA

The uncertainty and sensitivity analysis is performed with the software system SUSA (Software for Uncertainty and Sensitivity Analysis), developed at GRS /HOF 93/, /KRZ 94/, /KZR 03/, /KLO 08/. The aim of an uncertainty and sensitivity analysis is to provide quantitative information about the “lack of knowledge” or epistemic uncertainty of model results and to find out the major sources responsible for that uncertainty.

Such an analysis can be performed in a parametric and probabilistic form, i. e. all uncertainty sources must appropriately be represented by uncertain parameters and provided with adequate probability distributions which quantify the state of knowledge about the correct value of the parameter.

The principal steps of a probabilistic uncertainty and sensitivity analysis are:

- identify all possibly important sources of lack of knowledge uncertainty and represent them appropriately by uncertain parameters
- quantify the state of knowledge of the parameters by adequate probability distributions and, if necessary, quantify dependences among them
- generate a parameter sample according to the distributions and dependences specified before and perform the corresponding computer runs
- derive quantitative uncertainty statements on the model output and compute sensitivity measures from the results of the runs and the underlying parameter sample
- analyze and interpret the results.

The software system SUSA is organized according to the above structure and consists of several modules appropriate for the corresponding analysis step. The first SUSA-module is designed to support the analyst in converting the expert's state of knowledge about parameter values into adequate probability distributions and to appropriately express parameter dependence.

On the basis of this information the next module generates a multidimensional parameter sample, i. e. it randomly selects alternative parameter vectors from an appropriately constructed multivariable parameter probability distribution. Two types of

random selection procedures are offered, Simple Random Sampling (SRS) as well as Latin Hypercube Sampling (LHS). The SRS method is used in the present study because of the relatively small sample size (=100) needed. It is important to quantify the sampling error by calculating statistical tolerance limits, which is not possible with the LHS method.

Several statistical quantities can be used to formulate uncertainty statements on scalar output or for time-dependent model results. The most important of such quantities, particularly in applications with relatively small sample size N, are the so-called statistical tolerance intervals, i. e. the interval within which, with some confidence level, a specified proportion of a sampled population falls.

Sensitivity results for scalar output quantities can offer a variety of sensitivity measures which indicate how much the uncertainty of a parameter contributes to the uncertainty of the output quantity and thus can be used to establish a parameter uncertainty importance ranking.

For sensitivity analysis of time-dependent model output as considered in the present application the time-dependent sensitivity measures are computed and a time-dependent parameter uncertainty importance ranking is established.

4 Methods and Results

4.1 Parameter set

Only three of the input parameters for the MELODIE model, namely the **I**nstant **R**elease **F**raction (IRF), the dissolution rate and the inventory of I-129 were selected as parameters for the probabilistic analysis in order to limit the computation time of the MELODIE model including pre- and post-processing for 100 realizations. 100 model realizations were considered necessary in order to obtain robust results of the sensitivity analysis.

The **IRF** values are comprised between 6.8 % (minimum value) and 20.4 % (maximum value) of total activity contained in a canister /AND 05/. 8 % was applied as best estimate value /NF 05/. A triangular distribution was applied as probability density function (PDF), since no other information was available (Fig. 4.1).

The **dissolution rates [1/y]** of the spent fuel matrix are comprised between 1E-6 (minimum value for complete dissolution within 1 million years) and 2.5E-5 (maximum value) as selected in the calculation plan for deterministic calculations /AND 05/. 1E-05 was applied as best estimate value. A triangular distribution was applied as PDF, as before, since no other information was available (Fig. 4.2).

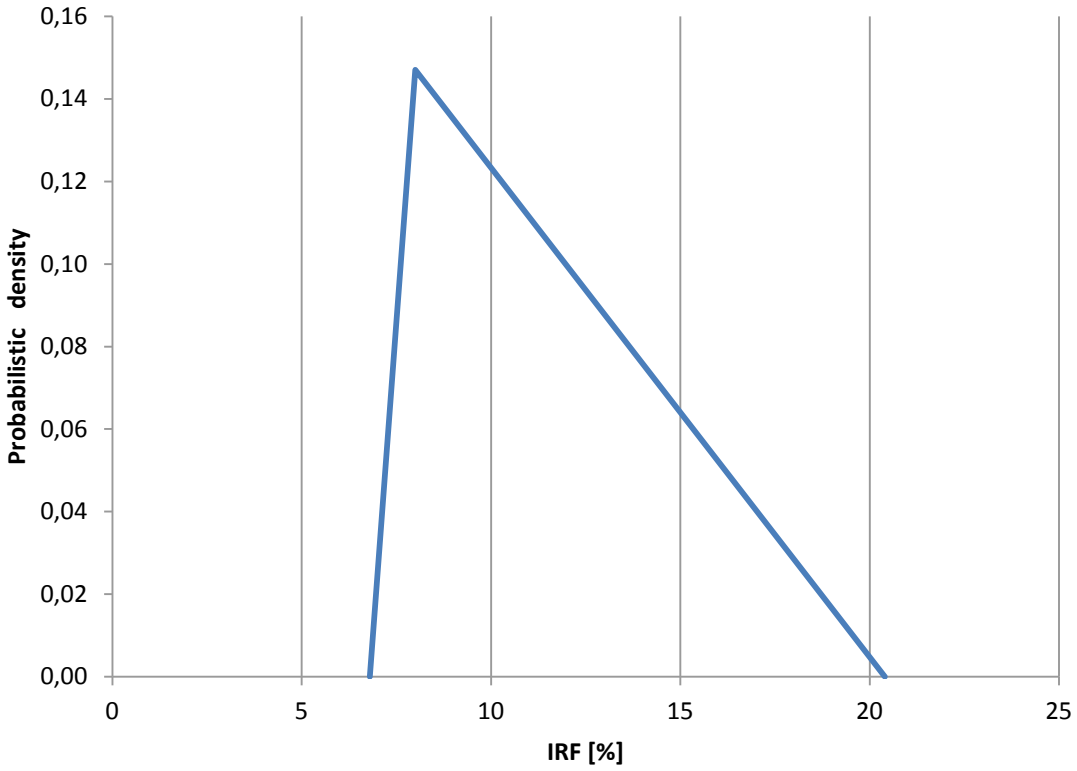

Fig. 4.1 Triangular Distribution of IRF

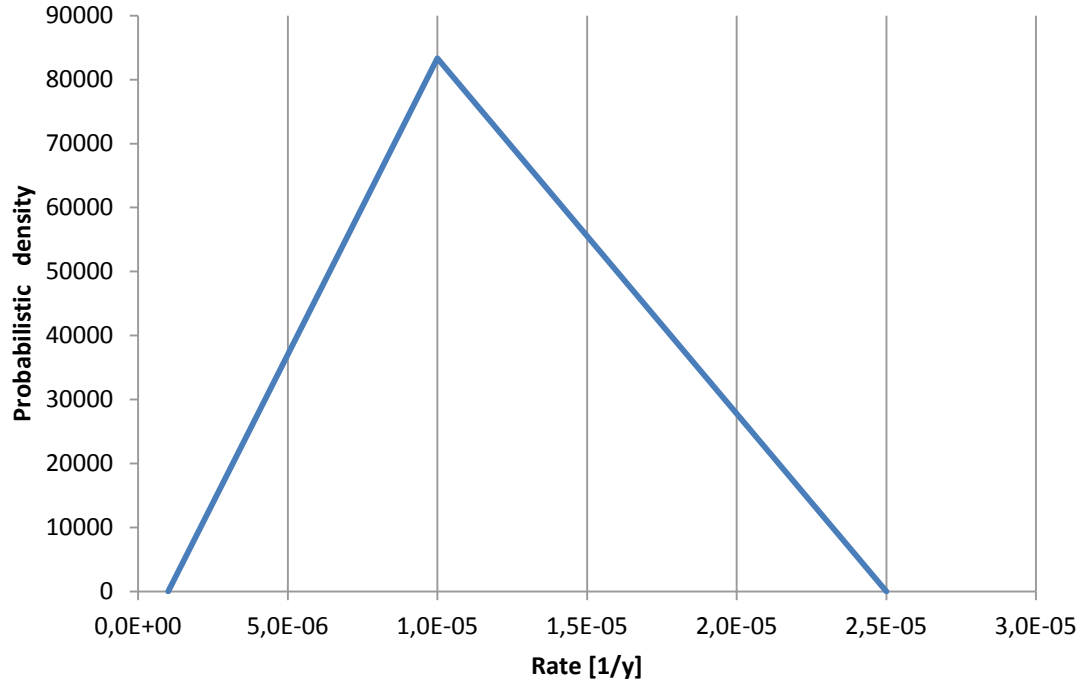

Fig. 4.2 Discrete Triangular distribution of dissolution rate

There were only discrete data available for the **^{129}I inventory [Bq/canister]**, since there are different UOX spent fuel canisters. The following discrete values were therefore related to the range and uncertainty of UOX spent fuel canisters disposed in the model. Total number of UOX spent fuel canisters is equal to 13 500. Of these canisters contain

- 27 % (3 645) 3.0E+09 Bq of ^{129}I (minimum value)
- 44 % (5 940) 3.6E+09 Bq of ^{129}I (median value)
- 29 % (3 915) 4.3E+09 Bq of ^{129}I (maximum value)

The PDF of the ^{129}I inventory was related to the percentage of canisters as depicted in the Fig. 4.3.

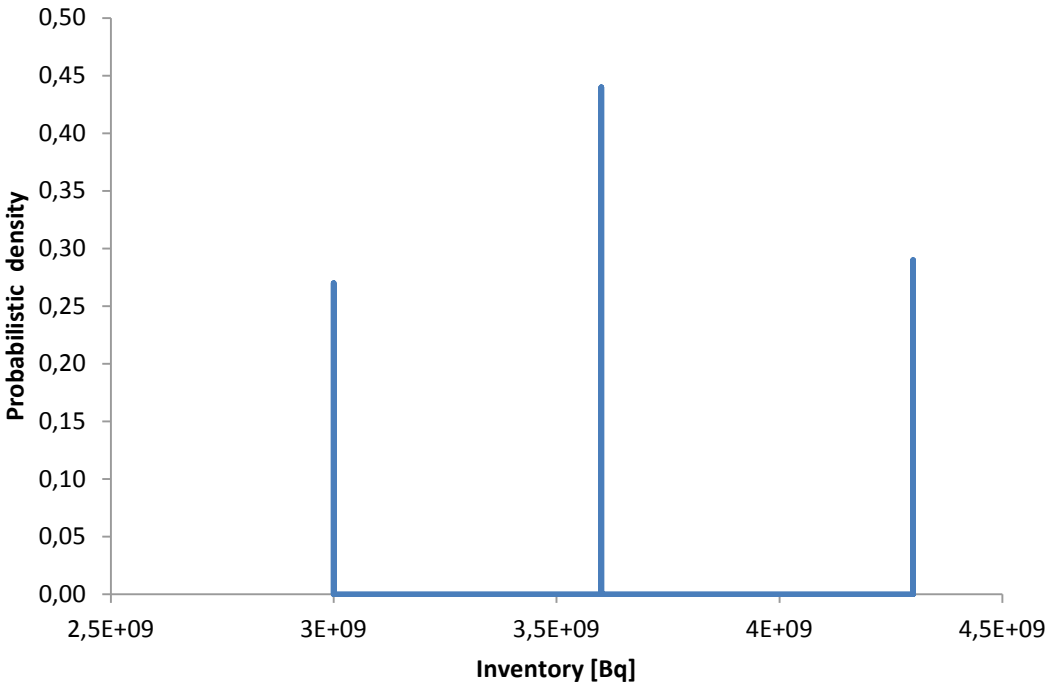

Fig. 4.3 Discrete distribution of inventory of ^{129}I

4.2 Input Data Set from SUSA for MELODIE

100 randomly selected parameter sets were generated by SUSA using the PDFs for the IRF, dissolution rate and the canister inventory. The complete set is listed in the appendix. The structure is shown in the Tab. 4.1. For each realization (Nr.) a value for the IRF, rate and canister inventory is provided.

Tab. 4.1 random data set

Nr.	IRF [%]	rate [1/y]	Canister Inventory [Bq]
1.	1.8013E+01	8.5042E-06	4.3000E+09
2.	1.1878E+01	1.7526E-05	3.0000E+09
3.	.....	.....	.....
.....			
100.	9.6202E+00	2.1930E-05	4.3000E+09

4.3 MELODIE calculations

The generated parameter sets were used as input for 100 simulation runs (realizations) using the MELODIE software and model.

Each calculation generates activity fluxes for the 4 indicators Phi1 to Phi4. The Fig. 4.4 to Fig. 4.7 show the activity fluxes over time of the 4 indicators calculated at the locations indicated in Fig. 2.3.

The activity flux to the host rock (Fig. 4.4[1]) and to the handling drift (Fig. 4.5) have similar shapes. The peak is in the first hundred years (certainly due to the IRF) and then decreases to a semi-plateau after 10 000 years since activity is released continuously by the canisters. When the release from the canisters terminates, the fluxes decrease sharply. The activity flux from the host rock at the top (Fig. 4.6) and the

[1] From Fig. 4.4 one could conclude that activitiy fluxes are becoming negative (not shown in the figure due to the logarithmic scale but in data file). The MELODIE software calculates the activity fluxes through the surface from a volume. A positive sign of the value of activity flux indicates that the activity flux is exiting the volume. A negative sign indicates that the activity flux is directed into the volume. The radionuclide transfer is driven by diffusion in the simulations and thus the transfer is governed by the concentration gradient. As long as activity can be released from the canisters, radionuclide concentrations are higher in the disposal tunnel than in the host rock. When the release from the canister is finished, the concentration gradient is reversed. In fact, the exit of disposal tunnel to the drift (indicator Phi 2) acts as a drain. The activity is transported back from the host rock to the canisters in order to exit via the disposal tunnel to the drift (Phi 2).

bottom (Fig. 4.7) results from diffusive flux as indicated by the late onset at approx. 70 000 y. It can be noticed that activity fluxes calculated at the top of the host rock are slightly higher than activity fluxes calculated at the bottom. This is due to the upward flow imposed in the model (Fig. 2.2).

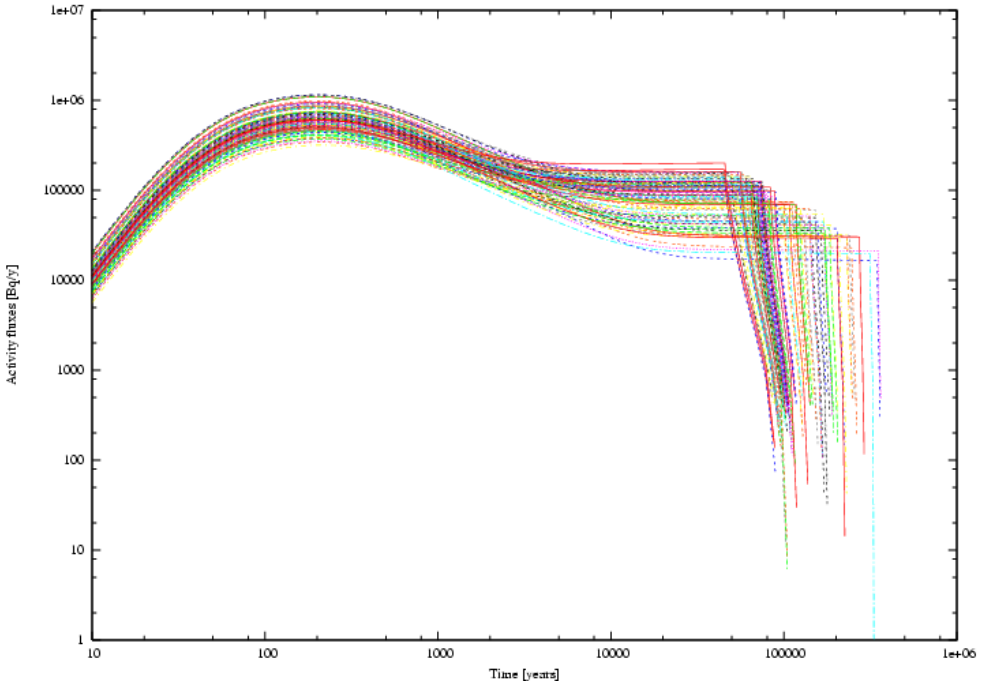

Fig. 4.4 Activity fluxes [Bq/y] calculated from disposal tunnel to the host rock (indicator Phi 1)

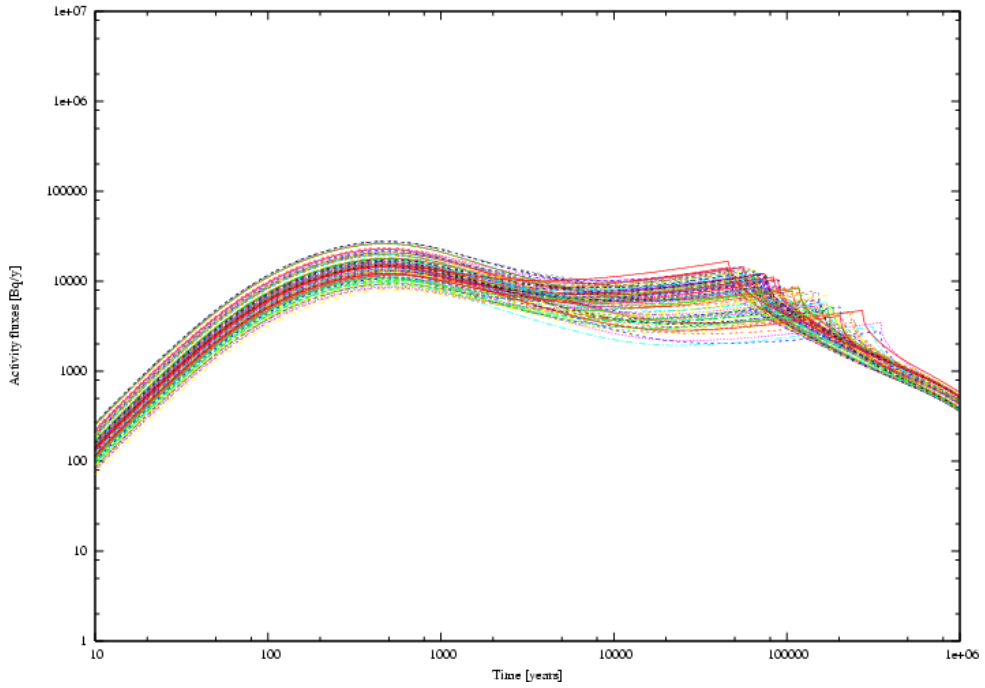

Fig. 4.5 Activity fluxes [Bq/y] calculated from disposal tunnel to the handling drift (indicator Phi 2)

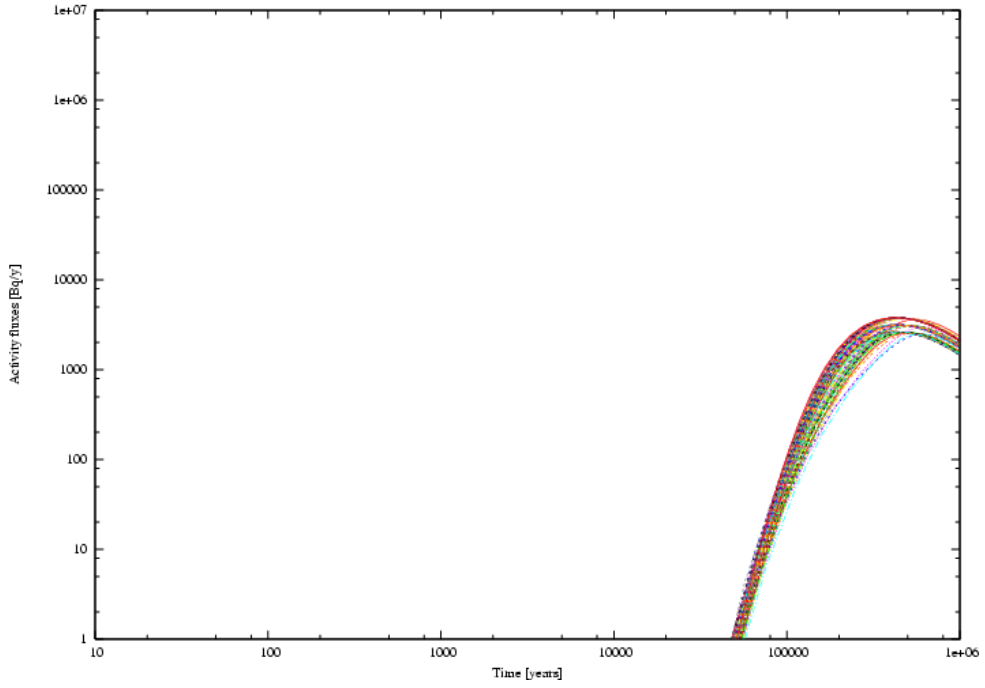

Fig. 4.6 Activity fluxes [Bq/y] calculated at the top of the host rock (indicator Phi 3)

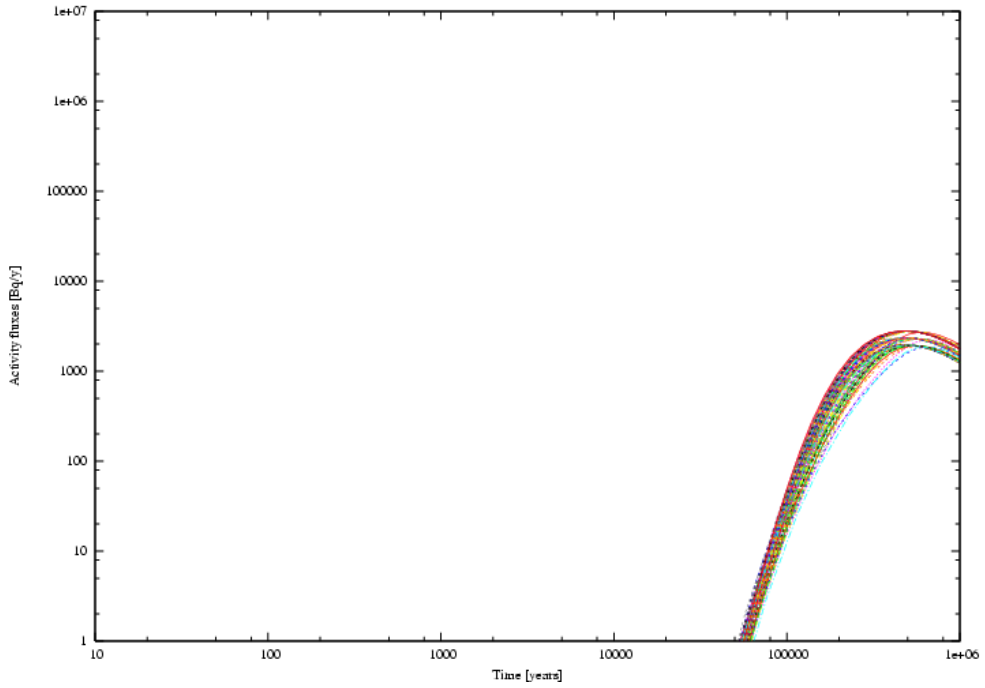

Fig. 4.7 Activity fluxes [Bq/y] calculated at the bottom of the host rock (indicator Phi 4)

4.4 Uncertainty and Sensitivity Analysis

The number of data points (time/activity flux) in each run of the MELODIE software was ranging from 89 to 93 since varying time steps were used by the MELODIE software in the 100 simulation runs. Therefore, a log-equidistant interpolation was done in SUSA on a logarithmic scale using 25 assigned times. As an internal control the Fig. 4.4 to Fig. 4.7 were successfully reproduced (not shown here).

4.4.1 Uncertainty

The uncertainty analysis comprised the calculation of the tolerance limits of the indicators Phi 1 to 4. The Fig. 4.8 to Fig. 4.11 represent the tolerance limits for the indicators Phi 1 to 4 in a confidence interval of 95 % (beta = 0.95) and a statement certainty of 95 % (gamma = 0.95). The sample size of 100 was higher than the necessary sample size of 93 for this statement. The uncertainty is only due to the uncertainty of the three model input parameters selected since all other input parameters and the model are fixed. The robustness of the results of SUSA on uncertainty is independent of the number of parameters.

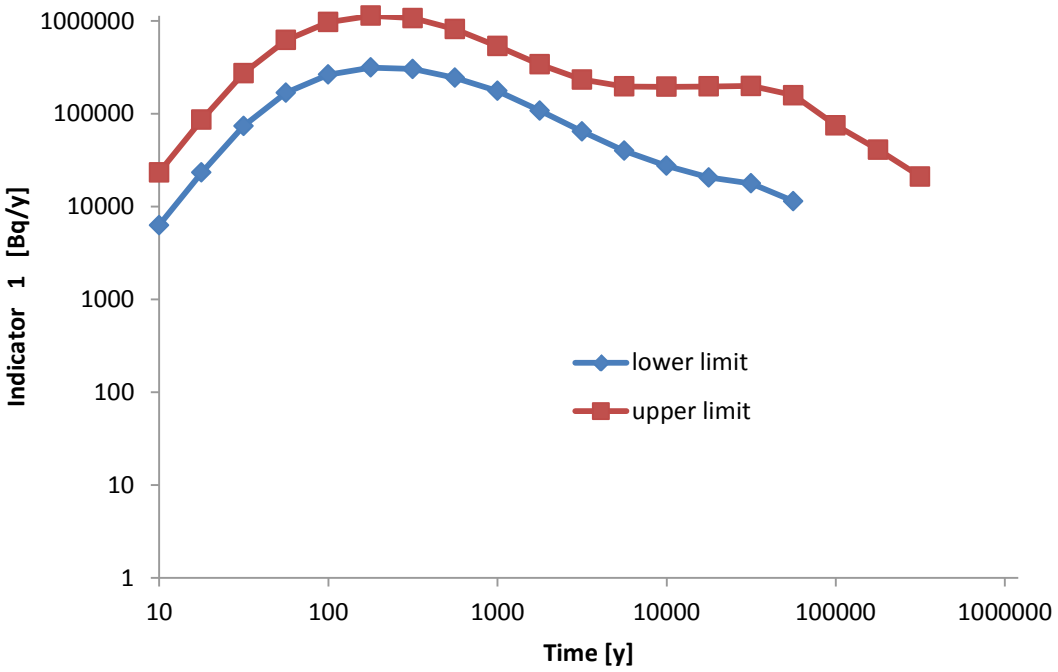

Fig. 4.8 Two-sided tolerance limits for Indicator Phi 1

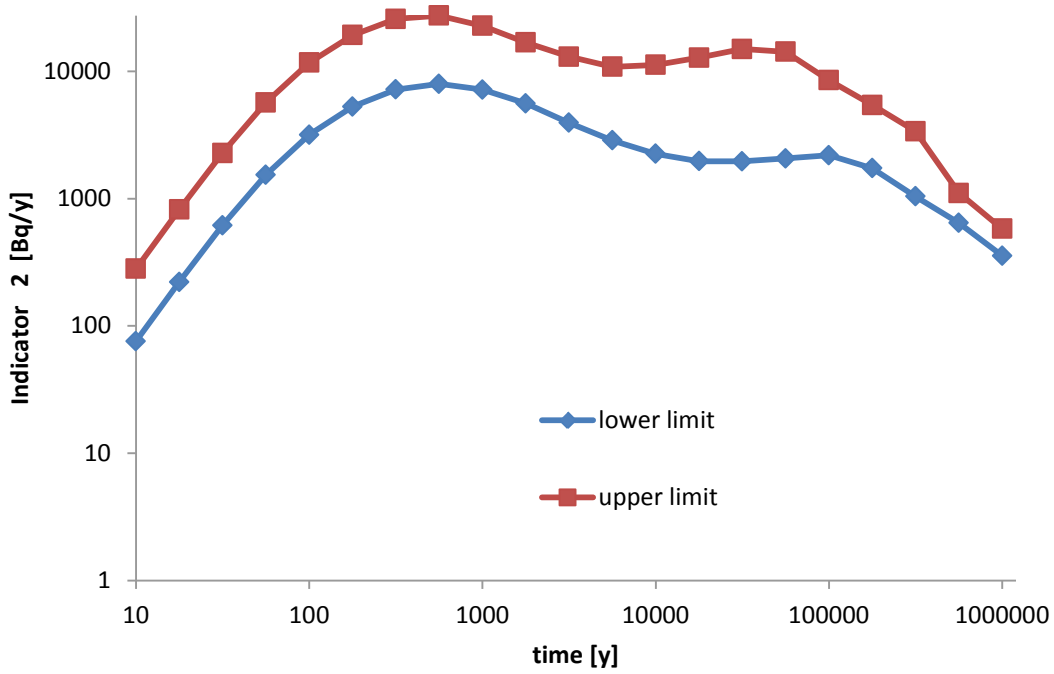

Fig. 4.9 Two-sided tolerance limits for Indicator Phi 2

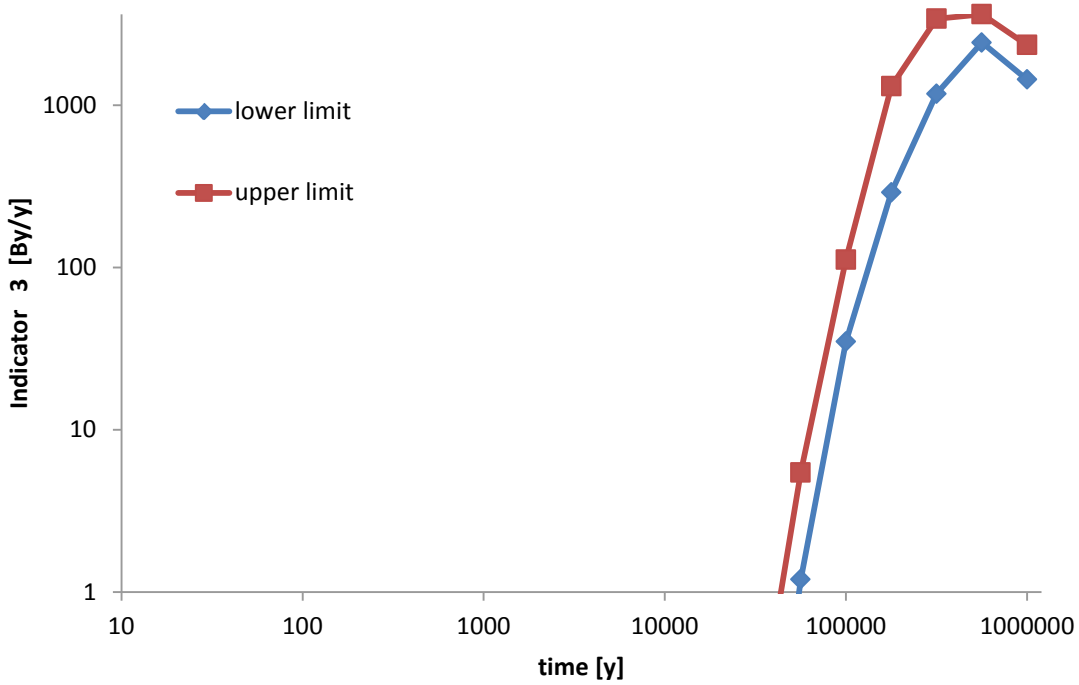

Fig. 4.10 Two-sided tolerance limits for Indicator Phi 3

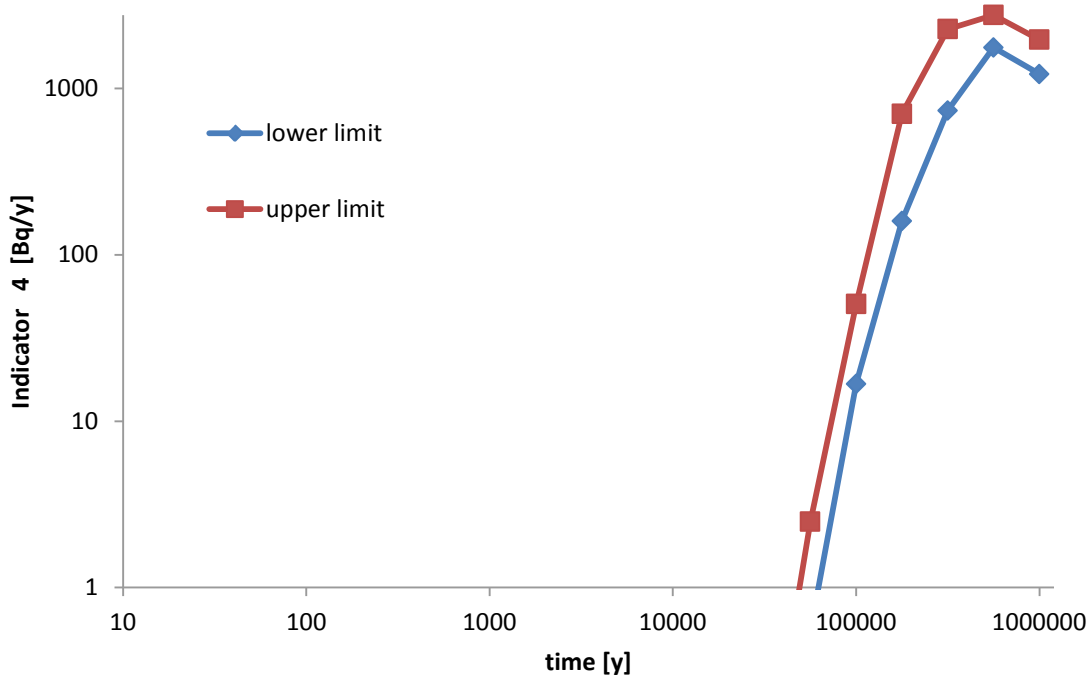

Fig. 4.11 Two-sided tolerance limits for Indicator Phi 4

4.4.2 Sensitivity

4.4.2.1 Time-dependent sensitivity analysis

The sensitivity analysis assesses the dependence of the uncertainty of the activity flux (i. e. one of the indicators) on the uncertainties of the parameters IRF, dissolution rate and inventory.

The coefficient of determination, R^2, is a measure of linear association between the model output — Indicator Phi 1, 2, 3, or 4 — and the total set of the three parameters. In the following the four indicators are discussed.

Indicator Phi 1 (activity flux into the host rock)

Starting with Indicator Phi 1, a value of almost unity of R^2 is calculated for all times $t < 32\,000$ y and for $t > 560\,000$ y (Fig. 4.12). During these periods the linear measure of the ordinary product moment correlation coefficient (see below) is able to provide a meaningful parameter sensitivity ranking. In the time window between 60 000 and 300 000 y the linear association between Indicator Phi 1 and the input parameters is poor. This time window corresponds to the transition period when the release from the canisters terminates and the fluxes drop to negligible values.

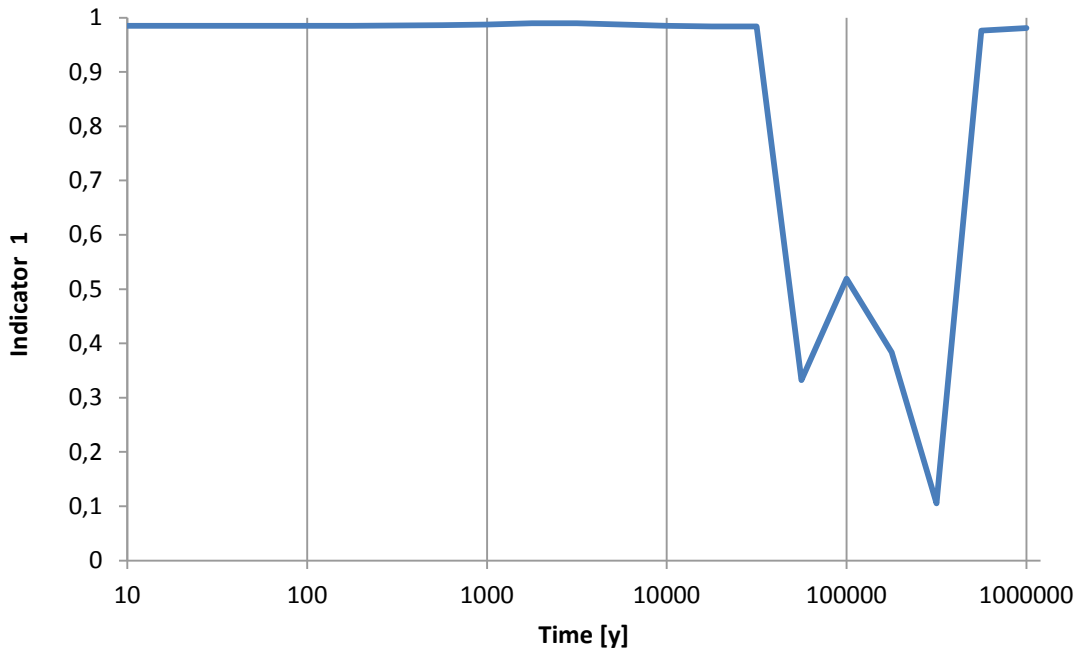

Fig. 4.12 The coefficient of determination R2 for indicator Phi 1

Fig. 4.13 shows the ordinary product moment correlation coefficients (CC) between Indicator Phi 1 (activity flux into the host rock) and the three parameters IRF (blue diamonds), dissolution rate (red squares) and inventory (green triangles). The CC is a measure of the degree of linear dependence between the input parameter (e. g. IRF) and the model output (Indicator Phi 1). An absolute CC value close to unity means an almost linear dependence. A positive (negative) value means that the output value tends to increase (decrease) with the value of the input parameter. In case of a high R^2 value (model can be well approximated by linear regression function) the absolute values of the CCs of the input parameters can be interpreted as a parameter sensitivity ranking.

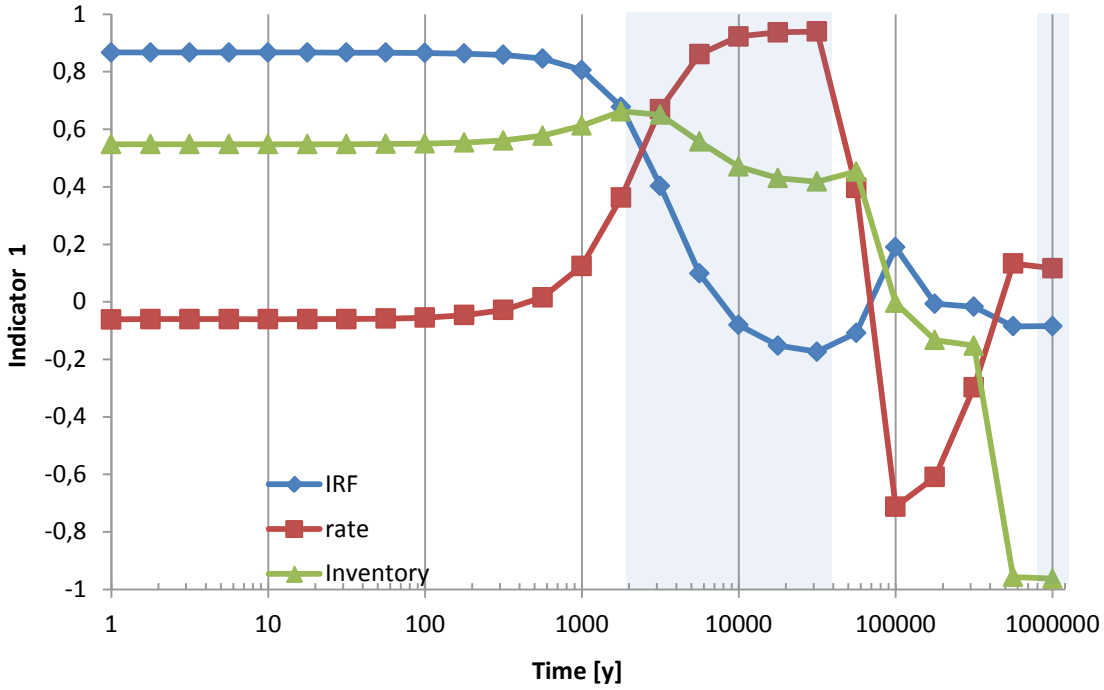

Fig. 4.13 Correlation coefficients (CCs) for indicator Phi 1

Fig. 4.13 shows further that the period of 1 Million years can be split into 4 distinct eras. The first era lasts from the beginning for approximately 2000 years and is dominated by the IRF (i. e. the uncertainty of Indicator Phi 1 is dominated by the uncertainty of the IRF) with a substantial (though smaller) influence by the Inventory. The second era lasts from approx. 3 000 to 30 000 years and is dominated by the dissolution rate with (again) a substantial influence by the inventory. The third era lasts from approx. 60 000 to 300 000 years and corresponds to the transition period mentioned before, where the R^2 parameter is unstable. The fourth era lasts from 500 000 years until the end of the calculations and is governed by the Inventory. The four eras, which are indicated in Figure 16 on the basis of their CC characteristics, are discussed in the following.

During the first era, the uncertainty of Indicator Phi 1 is mainly due to the uncertainty of the IRF. The uncertainty in the inventory is also relatively important, while the uncertainty of the dissolution rate plays no role at all. In this era the peak activity flux into the host rock occurs, which is due to the initial release of the nuclides (IRF ranging from 6.8 to 20.4 % of initial inventory with most likely values in the range 7 to 12 %). The time delay between nuclide release and activity flux passing into the host rock is short (of the order ~ 200 years as shown from the occurrence of the maximum in Fig. 4.4). It is clear that the continuous release of the nuclide (something between 0.01 %

and 0.25 % of initial inventory per century) is insignificant compared to the IRF in the first era. The first era ends after 2 000 years when the major part of the instantaneously released nuclide has left the disposal tunnel. Then the uncertainty of the continuously released nuclide gains importance.

During the second era, the uncertainty of Indicator Phi 1 is mainly due to the uncertainty of the dissolution rate. The uncertainty in the inventory is also relatively significant, while the uncertainty of the IRF plays no role anymore. In this era, the activity flux into the host rock comes from the continuous release of the nuclide, and a temporary equilibrium is reached between the continuous release and the activity flux into the rock. The dominance of the dissolution rate's uncertainty over the inventory's uncertainty can easily be understood by comparing the range of possible values of the dissolution rate (max/min = 25) with those of the inventory (max/min = 1.43). The second era ends after 30 000 years when the first canisters (with the highest rate) have finished releasing the nuclide.

The release of the nuclide from the canisters ends in the third era. This is the case at time $t = \frac{1 - IRF/100}{\text{rate}}$ for an individual canister in the model; t is in the range of 31 840 to 932 000 years with a best estimate value of 92 000 years. The correlation between Indicator Phi 1 and dissolution rate becomes negative at t (approx. 100 000 years). This can be explained by the following correlation: The **smaller** the dissolution rate, the **longer** takes the release and Indicator Phi 1 is **higher**.

During the fourth era, the uncertainty of Indicator Phi 1 is due to the uncertainty of the inventory, while the uncertainties of the IRF and of the dissolution rate are becoming unimportant. As explained in Sect. 4.3 however, Indicator Phi 1 is negative in this era (thus the negative CC). Therefore the physical process behind the finding (larger inventories lead to larger concentration gradients, irrespective of their direction) is of academic interest only; Indicator Phi 1 has lost its meaning as a performance indicator.

Indicator Phi 2

Indicator Phi 2 – the activity flux into the handling drift – shows a similar tendency as Indicator Phi 1. When comparing Fig. 4.14 and Fig. 4.15 with Fig. 4.12 and Fig. 4.13 from before it is obvious that the same distinct eras as before are revealed. The eras for Indicator Phi 2 start and end at a slightly later time than for Indicator Phi 1, which is probably due to the larger distance and thus nuclide travel time from the disposal

tunnel to the handling drift. The parameter sensitivity ranking is the same as in the case of Indicator Phi 1 and the same explanations hold again for Indicator Phi 2. The only significant difference in the pattern of the CCs is in the fourth era. The correlation with the inventory is now positive, which is due to the fact that Indicator Phi 2 is still positive in this era (while Indicator Phi 1 was negative).

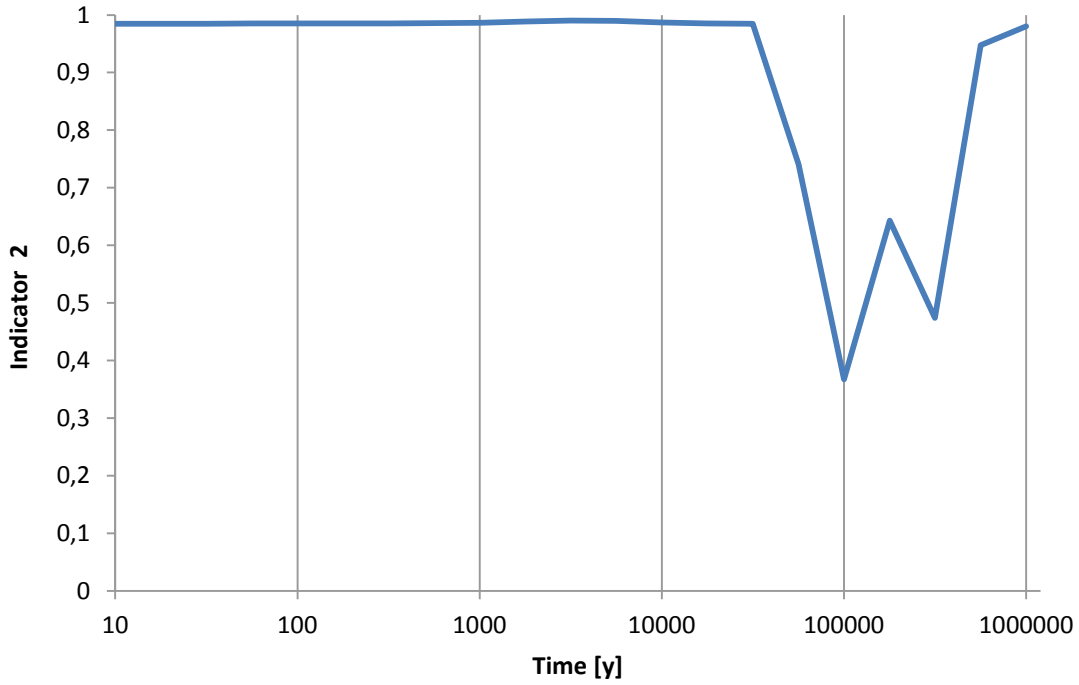

Fig. 4.14 The coefficient of determination R2 for indicator Phi 2

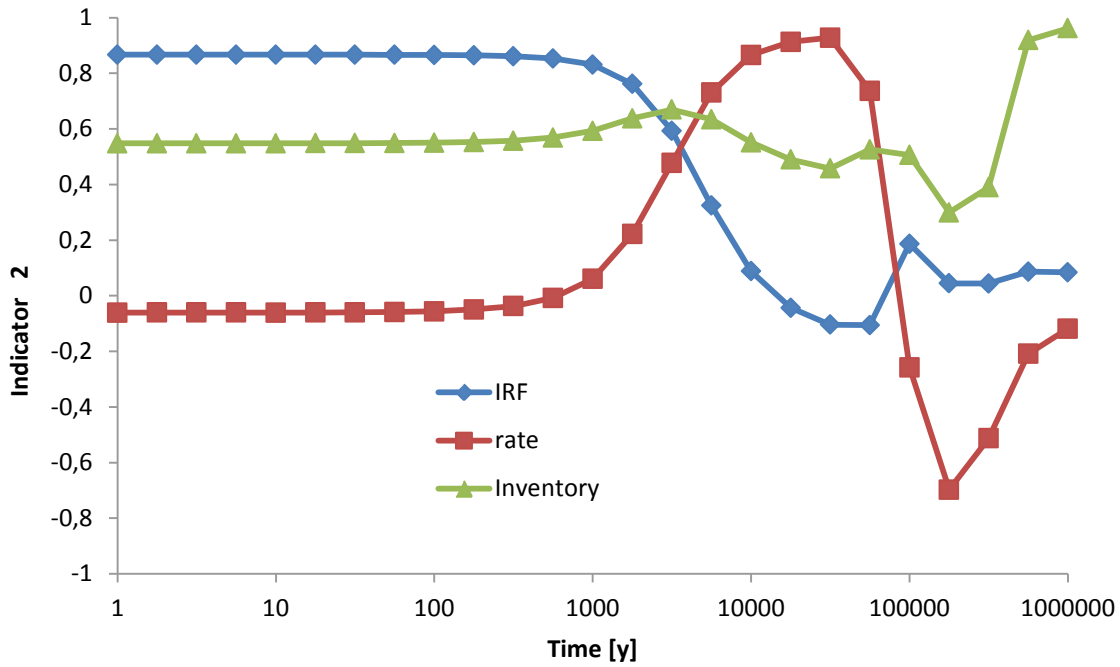

Fig. 4.15 Correlation coefficients (CCs) for indicator Phi 2

Indicator Phi 3

Indicator Phi 3 – the activity flux out from the host rock into the upper aquifer – has a high safety significance, because it indicates the activity that has passed all relevant safety barriers between the repository and the biosphere. Fig. 4.6 shows that it takes approx. 60 000 years until the first nuclide reach the top of the host rock by diffusive flux. The first canisters have stopped releasing the nuclide at this time.

Fig. 4.16 and Fig. 4.17 show the R^2 and the CC parameters of Indicator Phi 3 from 10 000 to 1 Million years. Due to the transfer time of the activity flux to the top surface of the host rock the parameters before 60 000 years are meaningless. R^2 is close to unity from 100 000 years onwards only.

The CC of the dissolution rate with Indicator Phi 3 is highest from 100 000 to 200 000 years. From 300 000 years onwards the inventory is again the most sensitive parameter. An intuitive explanation can be given on basis of the time lag of ~100 000 y between nuclide release and nuclide arrival in the aquifer: The uncertainty of the activity leaving the host rock between 100 000 and 200 000 y is determined by the uncertainty of the activity leaving the canisters between 0 and 100 000 y, which is governed by the dissolution rate. After 300 000 years, however, most of the canisters

finished the release of nuclides long before, so that the uncertainty of Indicator Phi 3 is determined by the uncertainty of the total activity in a canister, which depends only on the inventory.

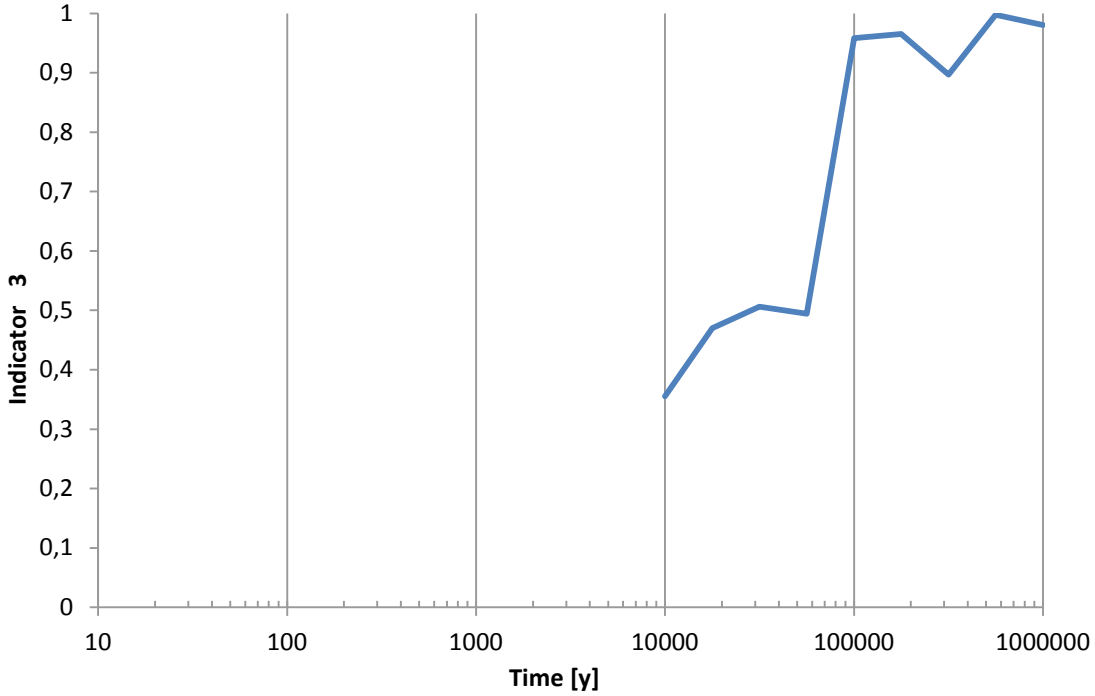

Fig. 4.16 The coefficient of determination R2 for indicator Phi 3

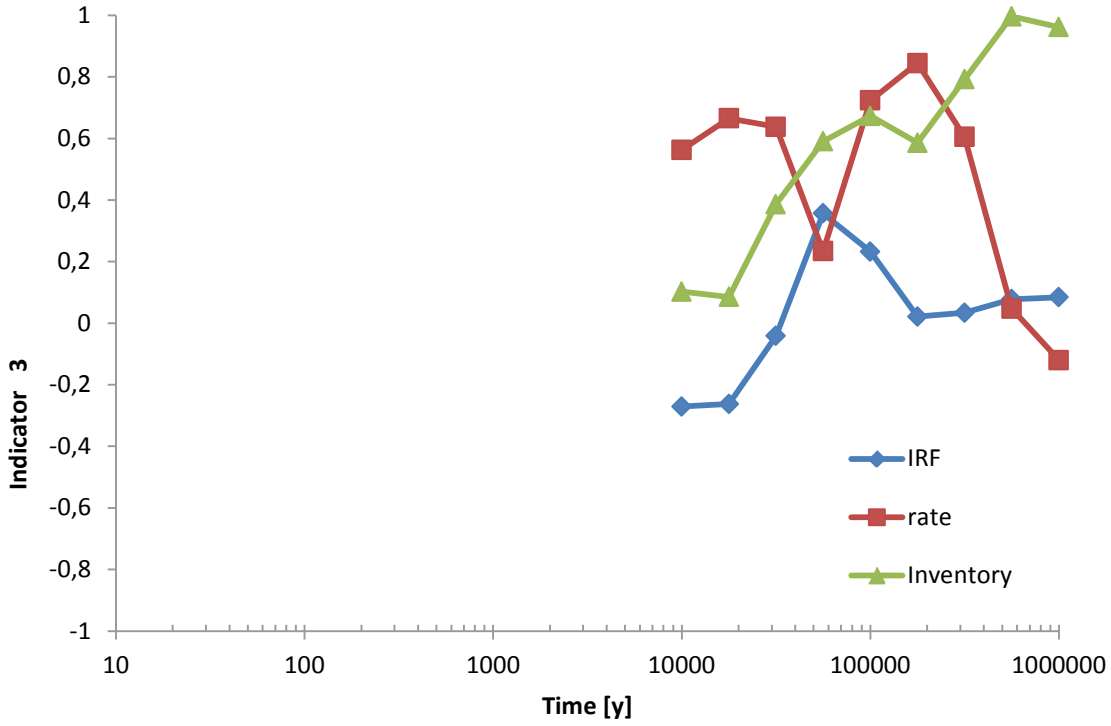

Fig. 4.17 Correlation coefficients (CCs) for indicator Phi 3

Indicator Phi 4

Indicator Phi 4 – the activity flux out from the host rock into the lower aquifer – has the same shape as Indicator Phi 3 (see Sect. 4.3). Therefore, the R^2 and the CC parameters of Indicator Phi 4 do not bring forth any new aspects regarding modeling results and are not discussed here.

4.4.2.2 Sensitivity analysis of the maximum flux

Fig. 4.18 shows the CCs between the maximum of the activity flux of Indicator Phi 1 ($I1_{max}$) and the three parameters IRF (1), dissolution rate (2) and Inventory (3).

The most sensitive parameter for $I1_{max}$ is the IRF and the least sensitive the dissolution rate. This is in accordance with the findings for the first era in Fig. 4.13, when the maximum occurs, and also the reason is the same: The maximum is due to the initial release of the nuclide. For a time span of a few hundred years the continuous nuclide release is negligible compared to the IRF. The inventory does have an influence on $I1_{max}$ of course, after all the total amount of nuclides released at t = 0 is the mere product of IRF and inventory. In addition, the sensitivity of the inventory on $I1_{max}$ is still

minor to the sensitivity of the IRF, because the range of the pdf of the inventory (max/min = 1.43) is much smaller than the range of the pdf of the IRF (max/min = 3.0).

The analysis of the maximum of Indicator Phi 2 (not shown) yields the same results as for Indicator Phi 1.

The most sensitive parameter for maximum of the activity flux of Indicator Phi 3 ($I3_{max}$) is the inventory (Fig. 4.20). This is not surprising, as the maximum of Indicator Phi 3 occurs sharply after 500 000 years, an era, when the inventory is the most sensitive parameter (in the time-dependent analysis, (Fig. 4.17).

The analysis of the maximum of Indicator Phi 4 (not shown) yields the same results as in the case of Indicator Phi 3.

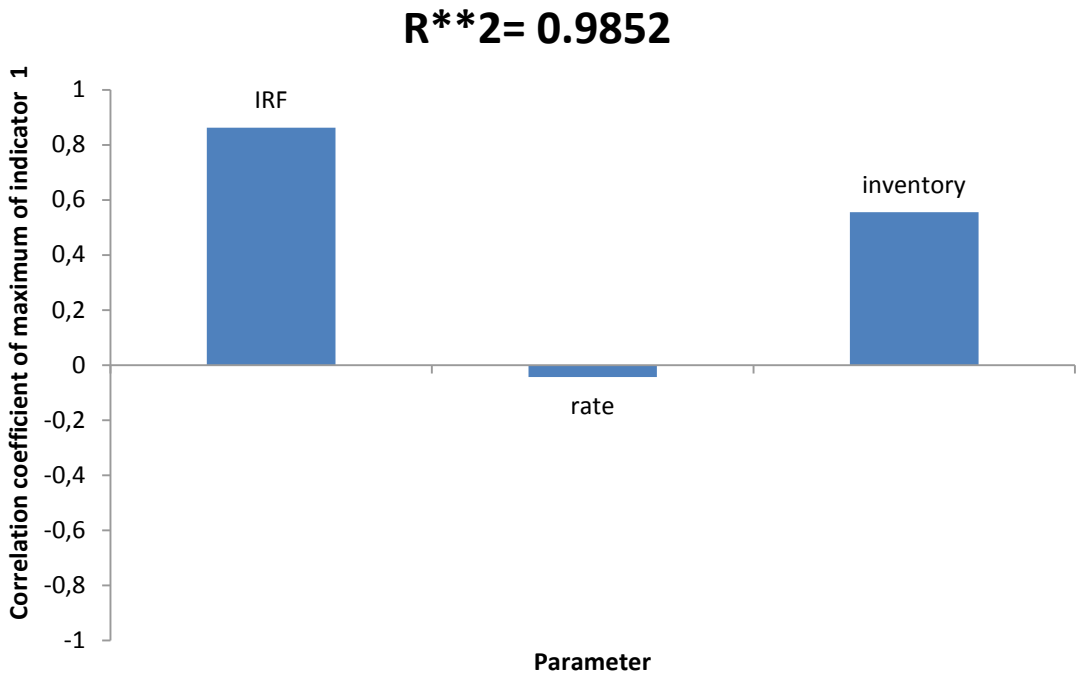

Fig. 4.18 The correlation coefficients between the 3 parameters and the maximum of indicator Phi 1

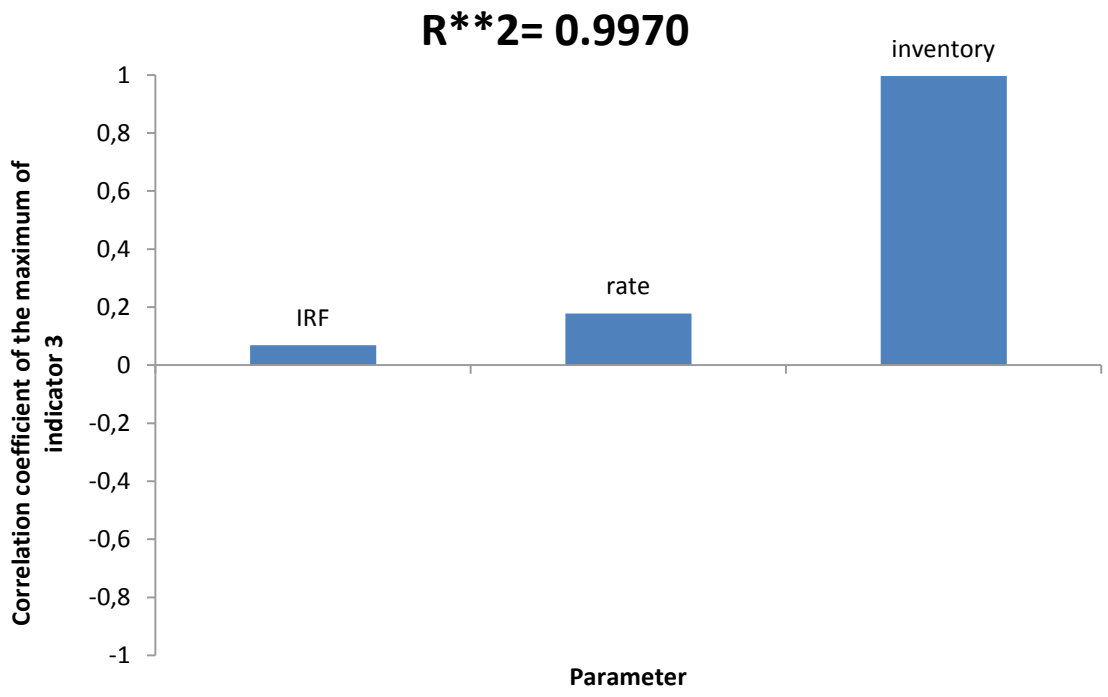

Fig. 4.19 The correlation coefficients between the 3 parameters and the maximum of indicator Phi 3

4.4.2.3 Sensitivity analysis of the time of maximum flux

Point of time for the maximum of Indicator Phi 1

The point of time for the maximum of Indicator Phi 1 is almost the same for all simulation runs (~ 200 y, cf. Fig. 4.4), i. e. within the parameter ranges chosen it does not depend much on any of the 3 parameters. This observation is coherent since it is known from Fig. 4.18 that the maximum itself does not depend on the dissolution rate (as it is far too small compared to the IRF). Since the maximum is a reflection of the initial release only, which occurs at t = 0 for all runs, and since the 3 parameters are unlikely to influence the transport processes of the nuclides, the time of the maximum should also be the same in all runs.

After these considerations it is surprising that the sensitivity analysis shows a clear dependency of the uncertainty of the point of time for the maximum on the uncertainties of the rate and the IRF (Fig. 4.20).

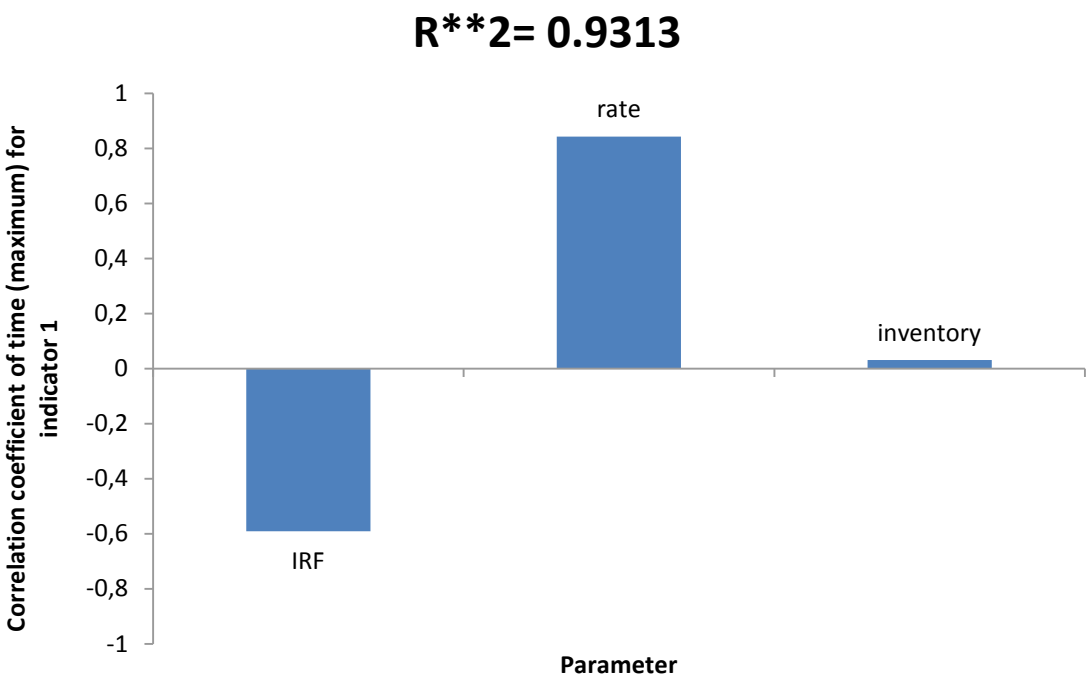

Fig. 4.20 The correlation coefficients between the 3 parameters and the point of time for maximum of indicator Phi 1

Therefore a closer look at the data is required: First of all, the uncertainty of the point of time for the maximum is indeed really small; it is ranging is from 204 to 211 years for the 100 runs. Within this range, high values (= late maxima) correlate with high resolution rates (CC = 0.84) and low IRFs (CC = –0.59). The physical interpretation is that with increasing fraction of the non-instantly released nuclides relative to the instantly released ones (by increasing rate or decreasing IRF) the maximum shifts to slightly later times compared to a pristine instant release event with rate = 0. So this effect – although very small – could be observed in the data.

However, there is also a numerical explanation of the finding, which becomes apparent when zooming into the original data around the maximum. The Fig. 4.21 shows that the time steps (~ 40 y) are too large to resolve the time range for the maximum of Indicator Phi 1. Apparently the values of the time steps and hence output times of the maximum, when the model is evaluated and results are calculated, depend directly or indirectly on the input parameters IRF and rate. This dependency (which depends on the software and not on the physical model) is reflected in the CC values calculated above.

A back reference to MELODIE confirms, that time steps are calculated automatically by the code and depend on the input parameters. Time steps are thus different from a calculation to another and cannot be set by the user.

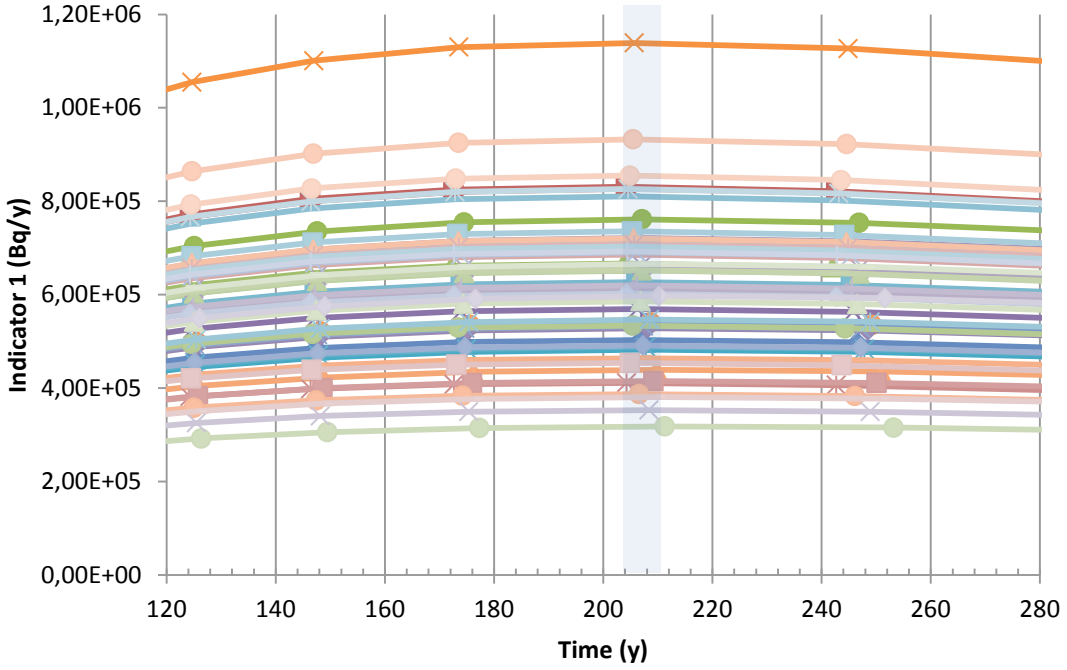

Fig. 4.21 Detail of the results of the simulation runs for indicator Phi 1 (zoom in on the maximum in Fig. 4.4)

This exercise is a good example of the possible shortcomings of simple interpretations of sensitivity analyses results. The data here does not provide information on the uncertainty of the point of time for the maximum of Indicator Phi 1, but indicates that the MELODIE software would need to be run with higher resolution (smaller time steps) around the point of time for the maximum, if this uncertainty was to be assessed.

Point of time for the maximum of Indicator Phi 3

The point of time for the maximum of Indicator Phi 3 falls between 390 000 and 630 000 years and this range is reasonably well resolved in time (typical time step size ~ 50 000 y). Hence in this case, the sensitivity analysis has a better chance to shed a light on physical processes rather than on computational subtleties.

Fig. 4.22 shows that the dissolution rate is the only parameter to which the point of time for the maximum of Indicator Phi 3 is sensitive: A smaller rate results in a later

maximum. It is interesting to note that the influence of the rate here is opposite to the case of Indicator Phi 1 described previously, where the CC between the rate and the point of time for the maximum was positive. The peak at Indicator Phi 1 reflects the pulse of the initial release, while the maximum of Indicator Phi 3 reflects the pulse of the complete release of activity from the canister (dependent on the inventory only). The influence of the dissolution rate on the point of time for the peak of Indicator Phi 1 was via *larger rate* = *larger quantity* (within a certain, short time window), while the influence of the rate on the point of time for the peak of Indicator Phi 3 is via *smaller rate* = *slower release* (of the finite quantity of the container).

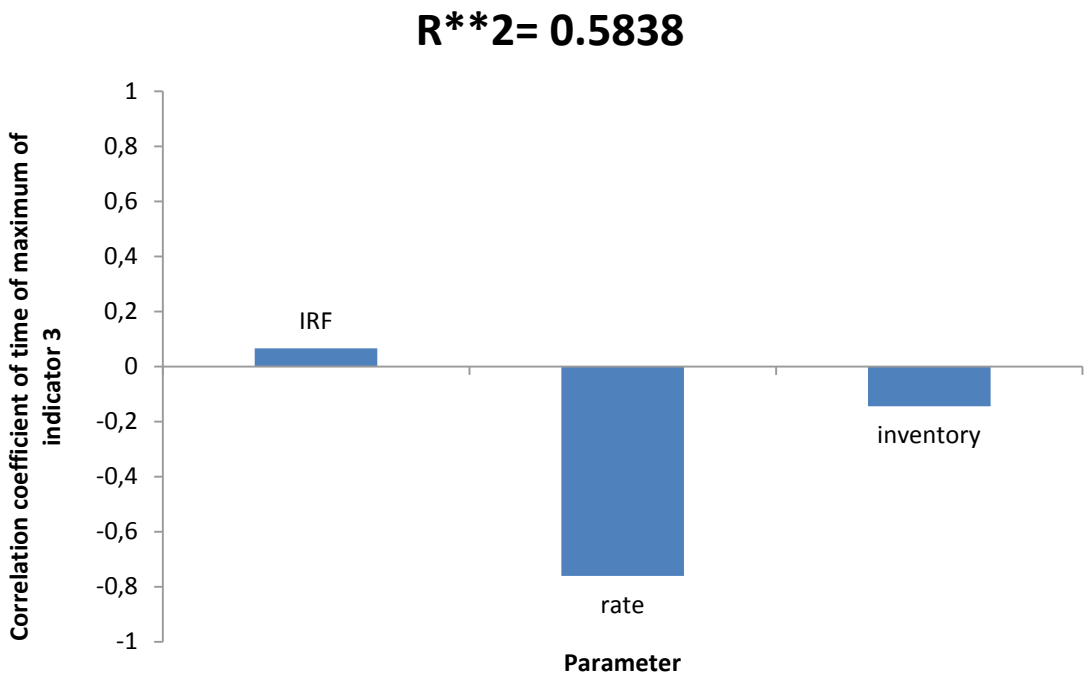

Fig. 4.22 The correlation coefficients between the 3 parameters and the point of time for maximum of Indicator Phi 3

4.4.2.4 Sensitivity analysis of the total release

One of the most important questions in a safety assessment of a repository is:

How much activity is released altogether out of the repository over the period of proof and what are the sensitive parameters?

This question is addressed in this study by summing up the total activity released out of the host rock (Indicator Phi 3 + Indicator Phi 4) over 1 Million years and dividing this number by the initial inventory. The resulting quantity is called here the e*scape fraction*. The division by the inventory (normalization) serves the purpose to go beyond the trivial result that the release will be higher if the initial inventory is higher and to assess the quality of the isolation function of the repository (which may or may not be sensitive to the Inventory). From Fig. 4.6 and Fig. 4.7 it is clear that the cut-off time of 1 Million years is still within the main pulse of activity flux, close to the point of time for its maximum. Hence the escape fraction may correlate with the time of the maximum of Indicator Phi 3: An earlier maximum may correlate with a higher escape fraction.

The escape fraction in the 100 simulation runs ranges from 29 % to 35 %. The CCs between the 3 parameters and the escape fraction are shown in Fig. 4.23: A higher dissolution rate correlates with a higher escape fraction.

This results looks like a mirrored version of Fig. 4.22: The higher the dissolution rate, the earlier is the maximum.

From this we can conclude, that the escape fraction is lowered and the maximum is delayed by a lower dissolution rate, which makes sense.

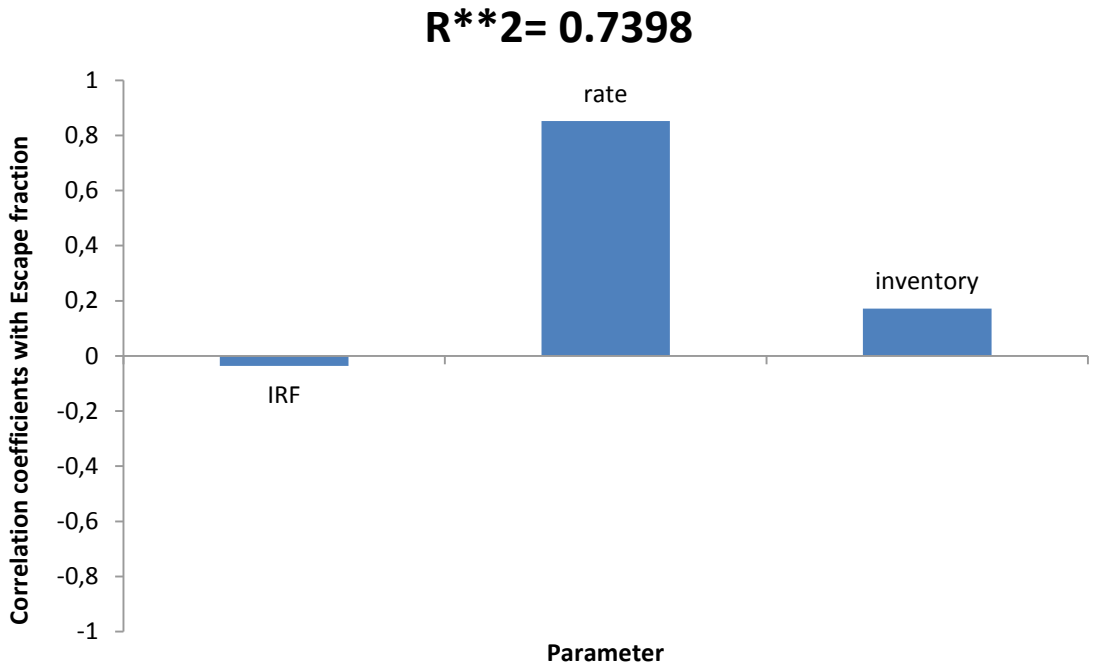

Fig. 4.23 The correlation coefficients between the 3 parameters and the escape fraction

5 Summary

Three input parameters (IRF, dissolution rate and inventory) were selected from the SF source term model for an uncertainty and sensitivity analysis. The probabilistic density functions were assigned and a parameter set for the probabilistic analysis was calculated. The resulting activity fluxes (indicators Phi 1 – 4) were calculated using the software MELODIE. The uncertainty and sensitivity analysis of the SF source term was performed with the SUSA software using the parameters and the activity fluxes and yielded the following results.

The uncertainties of the activity fluxes can be correlated to the uncertainties of the 3 selected parameters.

The time-dependent sensitivity analysis provided the coefficient of determination and the correlation coefficients for all parameters and activity fluxes. The activity flux from the tunnel to the host rock was assessed in detail and can be summarized as follows: The uncertainty of the IRF determines the uncertainty of the activity flux nearly linearly in the first era (< 2 000 years). The uncertainty of the dissolution rate determines the following era (3 000 – 30 000 years). The uncertainty of the inventory is determining the uncertainty of the activity flux of the last era (> 500 000 years).

The activity flux to the top of the host rock is only sensitive to the dissolution rate and the inventory. The transport time of the activity through the host rock may blur the influence of the IRF.

The maxima of the activity fluxes depend clearly on IRF (tunnel to host rock) and inventory (from the top of the host rock).

The definition of an escape fraction allowed a sensitivity analysis of the total release and led to the result that a lower dissolution rate lowers the total release of activity up to a certain cut-off time. A low dissolution rate helps lowering the overall release from the repository within one million years.

The impact of the IRF on the total release is hidden by the impact of the dissolution rate on it.

Numerical effects due to the resolution of time steps have to be watched and require a close look on data, model results and sensitivity analysis results to avoid misleading interpretations.

6 Conclusion

The SUSA analysis presented here led to important insights into the influence of the uncertainties of the SF source term parameters on the uncertainty of the activity flux out of the repository. However, in the present study the uncertainty and sensitivity analysis to be limited on a few selected parameters and a very simple model. The uncertainty and sensitivity analysis should be extended to more elaborated models and extended parameter sets in order to provide a more comprehensive picture of the parameters governing the overall repository performance.

References

/AND 05/ ANDRA : Dossier 2005: Argile, Synthèse de la faisabilité du stockage géologique en formation argileuse, ISBN: 2-9510108-8-5, 2005

/HOF 93/ Hofer E.: Probabilistische Unsicherheitsanalyse von Ergebnissen umfangreicher Rechenmodelle, GRS-A-2002, 1993.

/KLO 08/ Kloos M., Hofer E.: SUSA, The PC Version of the Software System for Uncertainty and Sensitivity Analysis of Results from Computer Models, User´s Guide and Tutorial, GRS mbH, 2008.

/KRZ 94/ Krzykacz B., Hofer E., Kloos M.: A software system for probabilistic uncertainty and sensitivity analysis of results from computer models, Proceedings of PSAM-II, San Diego, California, U.S.A., March, 1994.

/KZR 03/ Krzykacz-Hausmann B., Hofer E.: Quantifizierung von Modellunsicherheiten der PSA; GRS-A-3198, 2003.

/MAT 08/ Mathieu G., Dymitrowska M, Bourgeois M.: Modeling of radionuclide transport through repository components using finite volume element and multidomain methods, Physics and Chemistry of the Earth, 33, 216-224, 2008.

/NF 05/ NF-PRO: Phenomenological description. Reference concept spent fuel and HLW-Iron Canister-Granite, Deliverable D5.1.1 EC.

Table of figures

Appendix

Random data set generated by SUSA

```
Uncertainty and Sensitivity Analysis for Micado, I-129

 DATUM: 2008/12/11
 TIME:  10:58

 TYPE OF DESIGN: SIMPLE RANDOM

 NUMBER OF PARAMETERS                 =     3
 NUMBER OF FULLY DEPENDENT PARAMETERS =     0
 NUMBER OF FREE PARAMETERS            =     3
 SAMPLE SIZE                          =   100
 INITIAL DSEED =                 123457.0

================================================================

DISTRIBUTIONS OF THE PARAMETERS
================================

 PARAMETER NO.   1 : T R I A N G U L A R  DISTRIBUTION
                     BETWEEN   6.8000E+00 AND   2.0400E+01
                     WITH PEAK AT   8.0000E+00
----------------------------------------------------------------
 PARAMETER NO.   2 : T R I A N G U L A R  DISTRIBUTION
                     BETWEEN   1.0000E-06 AND   2.5000E-05
                     WITH PEAK AT   1.0000E-05
----------------------------------------------------------------
 PARAMETER NO.   3 : D I S C R E T E  DISTRIBUTION
                        POINTS   PROBABILITIES
                      3.0000E+09  2.7000E-01
                      3.6000E+09  4.4000E-01
                      4.3000E+09  2.9000E-01
----------------------------------------------------------------
================================================================

REQUIRED MEASURES OF ASSOCIATION BETWEEN FREE PARAMETERS
=========================================================

 PAR.1 PAR.2    MEASURE    TYPE
----------------------------------------------------------------

 CONTROL OF THE COMPUTATION OF THE CORRELATION
 OF THE TRANSFORMED NORMAL BY NUMERICAL INTEGRATION
 ( IF NECESSARY ) :
 MAXIMUM NUMBER OF ITERATIONS           =       20
 DESIRED ACCURACY OF ITERATION PROCEDURE=   2.5000E-02

P A R A M E T E R   V A L U E S   O F   T H E   D E S I G N
  RUN               INDEX OF PARAMETER
            1           2           3
     1   1.8013E+01   8.5042E-06   4.3000E+09
     2   1.1878E+01   1.7526E-05   3.0000E+09
     3   1.8930E+01   1.3020E-05   4.3000E+09
     4   1.0182E+01   2.8579E-06   3.6000E+09
     5   1.1115E+01   7.0427E-06   3.0000E+09
     6   8.7614E+00   5.3971E-06   3.6000E+09
     7   9.8980E+00   6.5405E-06   3.6000E+09
     8   1.6268E+01   8.9063E-06   4.3000E+09
     9   8.9737E+00   4.1554E-06   3.6000E+09
    10   1.5778E+01   3.6536E-06   4.3000E+09
    11   1.1024E+01   1.4324E-05   3.6000E+09
    12   1.4990E+01   1.1073E-05   4.3000E+09
    13   1.2824E+01   7.0484E-06   3.6000E+09
    14   1.2356E+01   1.4262E-05   4.3000E+09
    15   1.1082E+01   4.3294E-06   3.6000E+09
    16   1.1995E+01   1.5094E-05   3.6000E+09
    17   1.7626E+01   4.0443E-06   3.0000E+09
    18   9.7744E+00   1.9575E-05   3.0000E+09
    19   1.4261E+01   1.1311E-05   4.3000E+09
    20   1.7560E+01   5.7534E-06   3.0000E+09
    21   1.3996E+01   1.8510E-05   4.3000E+09
```

22	1.5367E+01	1.8298E-05	4.3000E+09
23	1.0361E+01	1.3166E-05	3.0000E+09
24	1.5199E+01	1.6426E-05	3.0000E+09
25	1.3144E+01	6.8776E-06	3.0000E+09
26	7.9998E+00	1.2445E-05	3.0000E+09
27	9.2763E+00	6.5524E-06	4.3000E+09
28	9.0282E+00	2.2237E-05	3.6000E+09
29	8.6847E+00	1.2156E-05	3.0000E+09
30	8.7059E+00	4.9262E-06	3.6000E+09
31	1.1593E+01	1.2621E-05	3.6000E+09
32	9.0155E+00	5.8646E-06	3.6000E+09
33	9.1964E+00	1.0048E-05	3.0000E+09
34	1.0118E+01	2.0234E-05	3.6000E+09
35	1.0156E+01	1.6586E-05	4.3000E+09
36	1.4420E+01	1.3058E-05	4.3000E+09
37	1.1924E+01	1.7902E-05	4.3000E+09
38	1.7999E+01	8.4673E-06	4.3000E+09
39	7.3563E+00	1.4342E-05	3.6000E+09
40	1.2870E+01	2.0693E-05	3.0000E+09
41	1.0291E+01	1.7153E-05	3.6000E+09
42	1.0370E+01	4.7824E-06	3.0000E+09
43	1.8913E+01	1.4071E-05	4.3000E+09
44	1.1023E+01	7.6734E-06	3.0000E+09
45	1.6624E+01	2.1182E-05	3.6000E+09
46	1.0399E+01	1.1974E-05	4.3000E+09
47	9.5268E+00	8.1123E-06	3.0000E+09
48	1.6450E+01	6.3766E-06	3.6000E+09
49	1.6240E+01	5.8677E-06	3.6000E+09
50	1.3245E+01	1.5896E-05	3.6000E+09
51	1.4844E+01	1.9728E-05	3.6000E+09
52	1.0549E+01	1.3105E-05	3.6000E+09
53	1.1245E+01	1.7250E-05	3.0000E+09
54	1.8699E+01	1.6514E-05	4.3000E+09
55	1.1781E+01	1.4210E-05	3.0000E+09
56	1.6401E+01	5.4365E-06	3.6000E+09
57	1.5816E+01	2.8839E-06	3.0000E+09
58	1.1135E+01	1.1316E-05	3.6000E+09
59	9.4929E+00	1.3944E-05	3.6000E+09
60	8.7651E+00	1.5339E-05	4.3000E+09
61	8.8018E+00	1.3335E-05	4.3000E+09
62	1.3608E+01	8.5946E-06	4.3000E+09
63	1.0638E+01	1.5885E-05	4.3000E+09
64	8.5888E+00	1.3510E-05	4.3000E+09
65	1.4736E+01	1.4402E-05	3.0000E+09
66	1.0162E+01	2.1787E-05	3.0000E+09
67	1.0369E+01	1.4023E-05	3.6000E+09
68	9.7406E+00	3.1783E-06	3.0000E+09
69	8.7808E+00	5.8852E-06	4.3000E+09
70	1.1792E+01	1.3655E-05	4.3000E+09
71	1.3361E+01	7.1300E-06	4.3000E+09
72	1.0852E+01	1.4492E-05	3.0000E+09
73	1.1492E+01	1.5514E-05	3.0000E+09
74	8.0181E+00	1.5393E-05	3.6000E+09
75	1.0637E+01	1.3615E-05	4.3000E+09
76	1.0819E+01	1.3845E-05	4.3000E+09
77	1.0599E+01	1.8181E-05	3.6000E+09
78	7.5679E+00	7.9889E-06	3.6000E+09
79	1.1625E+01	1.5070E-05	4.3000E+09
80	1.3457E+01	1.0018E-05	3.6000E+09
81	1.5438E+01	7.5528E-06	3.0000E+09
82	1.1972E+01	9.2962E-06	3.6000E+09
83	1.7348E+01	1.2247E-05	3.0000E+09
84	1.4133E+01	1.1085E-05	3.6000E+09
85	1.3527E+01	1.2938E-05	3.6000E+09
86	1.6654E+01	1.4443E-05	3.0000E+09
87	7.3100E+00	1.8682E-05	3.0000E+09
88	1.4558E+01	1.4811E-05	3.0000E+09
89	1.3871E+01	4.2926E-06	3.6000E+09
90	1.5324E+01	1.1894E-05	4.3000E+09
91	1.4256E+01	4.9077E-06	3.0000E+09
92	1.0720E+01	5.7777E-06	3.0000E+09
93	1.1438E+01	1.3716E-05	3.6000E+09
94	8.2121E+00	1.3652E-05	3.0000E+09
95	1.9529E+01	9.5935E-06	3.0000E+09
96	1.6828E+01	9.2785E-06	3.6000E+09
97	1.6395E+01	6.0840E-06	3.0000E+09
98	7.3458E+00	1.5293E-05	3.6000E+09

```
   99   1.0818E+01   1.7549E-05   4.3000E+09
  100   9.6202E+00   2.1930E-05   4.3000E+09

NUMBER OF DESIGN REPETITIONS DUE TO PAR. RESTRICT.=     0
LAST DSEED=         1925803439.0

DESIGN HAS BEEN GENERATED
AND WRITTEN ON OUTPUT FILE
LAST DSEED=         1925803439.0
```

Gesellschaft für Anlagen- und Reaktorsicherheit (GRS) mbH

Schwertnergasse 1
50667 Köln
Telefon +49 221 2068-0
Telefax +49 221 2068-888

Forschungszentrum
85748 Garching b. München
Telefon +49 89 32004-0
Telefax +49 89 32004-300

Kurfürstendamm 200
10719 Berlin
Telefon +49 30 88589-0
Telefax +49 30 88589-111

Theodor-Heuss-Straße 4
38122 Braunschweig
Telefon +49 531 8012-0
Telefax +49 531 8012-200

www.grs.de

ISBN 978-3-939355-93-9